

Lattice-Boltzmann Simulations of Fluid Flows in MEMS

Xiaobo Nie,¹ Gary D. Doolen,² and Shiyi Chen^{1,4}

Received April 14, 2001; accepted November 20, 2001

The lattice Boltzmann model is a simplified kinetic method based on the particle distribution function. We use this method to simulate problems in MEMS, in which the velocity slip near the wall plays an important role. It is demonstrated that the lattice Boltzmann method can capture the fundamental behaviors in micro-channel flow, including velocity slip, nonlinear pressure drop along the channel and mass flow rate variation with Knudsen number. The Knudsen number dependence of the position of the vortex center and the pressure contour in micro-cavity flows is also demonstrated.

KEY WORDS: Lattice-Boltzmann; microfluid; velocity slip.

1. INTRODUCTION

The development of technologies in Micro-electro-mechanical systems (MEMS) has motivated the study of fluid flows in devices with micro-scale geometries, such as micro-channel and micro-cavity flows.⁽¹⁾ In these flows, the molecular mean free path of the fluid molecules could be the same order as the typical geometric dimension of the device and the continuum hypothesis which is the fundamental for the Navier–Stokes equation breaks down. An important feature in these flows is the emergence of a slip velocity at the flow boundary, which strongly affects the mass and heat transfer in the system. In micro-channel experiments, it has been observed that the

¹ Department of Mechanical Engineering, The Johns Hopkins University, Baltimore, Maryland 21218.

² Center for Nonlinear Studies and Theoretical Division, Los Alamos National Laboratory, Los Alamos, New Mexico 87545.

³ National Key Laboratory for Turbulence Research, Peking University, People's Republic of China.

⁴ To whom correspondence should be addressed; e-mail: syc@taylor.me.jhu.edu

measured mass flow rate is higher than that based on a non-slip boundary condition.⁽²⁾ The Knudsen number, $K_n = l/H$, can be used to identify the influence of the effects of the mean free path on these flows, where l is the mean free path of the molecules and H is a typical dimension of the flow domain. It has been pointed out⁽³⁾ that for a system with $K_n < 0.001$, the fluid flow can be treated as continuum. For $K_n > 10$ the system can be considered as a free-molecular flow. The fluid flow for $0.001 < K_n < 10$, which often appears in the MEMS, can not be treated as a continuum flow or a free-molecular flow. Traditional kinetic methods, such as molecular dynamics simulations⁽⁴⁾ and the continuum Boltzmann equation, could be used to describe these flows. But these methods are more complicated than schemes usually used for continuum hydrodynamic equations. The solution of the Navier–Stokes equation including the velocity-slip boundary condition with a variable parameter has also been used to simulate micro-channel flows.⁽⁵⁾

In the past ten years, the lattice Boltzmann method (LBM)⁽⁶⁾ has emerged as an alternative numerical technique for simulating fluid flows. This method solves a simplified Boltzmann equation on a regular lattice. The solution of the lattice Boltzmann equation converges to the Navier–Stokes solution in the continuum limit (small Knudsen number). In addition, since the lattice Boltzmann method is intrinsically kinetic, it can be also used to simulate some fluid flows with high Knudsen numbers, including fluid flows in very small MEMS.

2. A LATTICE BOLTZMANN MODEL FOR MICRO-FLOWS

To demonstrate the utility of LBM, we use the D2Q9 model⁽⁷⁾ with three speeds and nine velocities on a two-dimensional square lattice. The velocities, \mathbf{c}_i , include eight moving velocities along the links of the square lattice and a zero velocity for the rest particle. They are: $(\pm 1, 0)$, $(0, \pm 1)$, $(\pm 1, \pm 1)$, $(0, 0)$. Let $f_i(\mathbf{x}, t)$ be the distribution functions at \mathbf{x} , t with velocity \mathbf{c}_i . The lattice Boltzmann equation with the BGK collision approximation^(7,8) can be written as

$$f_i(\mathbf{x} + \mathbf{c}_i \delta t, t + \delta t) - f_i(\mathbf{x}, t) = -\frac{f_i - f_i^{\text{eq}}}{\tau} \quad (1)$$

where f_i^{eq} ($i = 0, 1, \dots, 8$) is the equilibrium distribution function and τ is the relaxation time. We have assumed that the spatial separation of the lattice is δx and the time step is δt . A suitable equilibrium distribution is:⁽⁷⁾

$$f_i^{\text{eq}} = t_i \rho \left[1 + \frac{c_{i\alpha} u_\alpha}{c_s^2} + \frac{(c_{i\alpha} c_{i\beta} - c_s^2 \delta_{\alpha\beta})}{2c_s^4} u_\alpha u_\beta \right] \quad (2)$$

Here $c_s = 1/\sqrt{3}$ is the sound speed, $t_0 = 4/9$, $t_1 = t_2 = t_3 = t_4 = 1/9$ and $t_5 = t_6 = t_7 = t_8 = 1/36$. The Greek subscripts α and β denote the spatial directions in Cartesian coordinates. The density ρ and the fluid velocity \mathbf{v} are defined by $\rho = \sum_i f_i$, $\rho\mathbf{v} = \sum_i \mathbf{c}_i f_i$. In previous lattice-BGK models, τ was chosen to be a constant. This is applicable only for nearly-incompressible fluids. In micro-flows, the local density variation is still relatively small, but the total density changes, for instance the density difference between the inlet and exit of a very long channel could be quite large. To include the dependence of viscosity on density we replace τ in Eq. (1) by τ' :

$$\tau' = \frac{1}{2} + \frac{1}{\rho} \left(\tau - \frac{1}{2} \right) \quad (3)$$

As shown later in Eq. (7), this makes the dynamic viscosity $\mu = \rho\nu$ constant which is required for most realistic fluids. Using the Chapman–Enskog multi-scale expansion technique,⁽⁶⁾ we obtain the following Navier–Stokes equations in the limit of long wavelength, low frequency and small Mach number:

$$\partial_t \rho + \partial_\alpha (\rho u_\alpha) = 0 \quad (4)$$

$$\partial_t (\rho u_\alpha) + \partial_\beta (\rho u_\alpha u_\beta) = -\partial_\alpha P + \partial_\beta \pi_{\alpha\beta} \quad (5)$$

$$P = c_s^2 \rho, \quad \pi_{\alpha\beta} = \nu (\partial_\alpha (\rho u_\beta) + \partial_\beta (\rho u_\alpha)) \quad (6)$$

where

$$\nu = c_s^2 (2\tau - 1) / (2\rho) \quad (7)$$

is the kinematic viscosity.

In classical kinetic theory, the viscosity ν for a hard sphere gas is linearly proportional to the mean free path. Similarly, we define the mean free path l in the LBM as: $a(\tau - 0.5)/\rho$, where a is a constant which will be determined by comparing simulation results with experiments in the following micro-channel flow simulation. The factor 0.5 comes from the finite difference scheme used in the lattice Boltzmann discretization for the discrete Boltzmann equation.⁽⁶⁾ Therefore, we have the relation between the Knudsen number and the relaxation parameter:

$$K_n = \frac{a(\tau - 0.5)}{\rho H}$$

3. SIMULATION RESULTS AND DISCUSSION

Our first numerical example is the micro-channel flow⁽²⁾ where the flow is contained between two parallel plates separated by a distance H and driven by the pressure difference between the inlet pressure, P_i , and the exit pressure, P_e . The channel length in the longitudinal direction is L . We take $L = 1000$, $H = 10$ (lattice units) in our simulations, satisfying $L/H \gg 1$ consistent with most experimental conditions. The bounce-back wall boundary condition is used for the particle distribution functions at the top and bottom plates, i.e., when a particle distribution moves to a wall, the particle distribution scatters back to the fluid node opposite to its incoming direction. The bounce-back boundary condition of particle distribution will result in a non-slip boundary condition of average velocity in the continuous limit ($K_n \ll 1$). However, when K_n is not very small, the continuous assumption does not hold, resulting in a mean slip velocity on wall boundary. This is because of the kinetic nature of the lattice-Boltzmann method. In our simulation, the solid wall is set between two mesh layers. For example, when $H = 10$, the y -coordinates of the fluid nodes are $y = 0.5, 1.5, \dots, 9.5$. A pressure boundary condition is used at the input and the exit. The pressure boundary condition is set by extrapolation method⁽⁹⁾ in which the particle distribution functions in the input and the exit are calculated based on the given pressures on these boundaries.

It is customary to define the slip velocity V_s for the micro-channel using the following formula:

$$u(y) = u_0(Y - Y^2 + V_s) \quad (8)$$

where $u(y)$ is the x -direction velocity, u_0 and V_s can be obtained by fitting the numerical results to Eq. (8) using the least square method. This definition of the slip velocity is consistent with others.^(2,5) The profiles of normalized velocity, $V = u(y)/u_0$, at the exit of the channel are shown in Fig. 1 for various Knudsen numbers which are defined based on the width of the channel when the pressure ratio $\alpha = P_i/P_e = 2$. The velocity distributions are well fitted by Eq. (8), demonstrating that high Knudsen flows can be well approximated by parabolic velocity distributions with slip boundary velocity. It is evident that the slip velocity increases as a function of Knudsen number. In Fig. 2, we plot the slip velocity V_s and the normalized mass flow rate $M_f = M/M_0$, as functions of Knudsen number. The normalization factor, $M_0 = \frac{h^3 P_e}{24\nu L} (\alpha^2 - 1)$, is the mass flow rate when the slip velocity is zero. To calculate the Knudsen number we have chosen $a = 0.388$ to best match the simulated mass flow rate with experiments (see the theoretical curve in Fig. 5). In general, the parameter a should depend

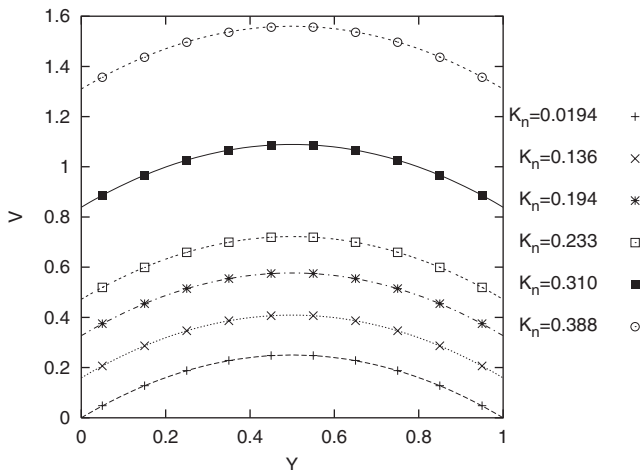


Fig. 1. The profiles of normalized velocity $V = u/u_0$ at the exit of a micro-channel flow for various Knudsen number K_n .

on the interaction force between fluid and wall and should not depend on flow conditions. Using a least square fit to the data in Fig. 2, we obtain the dependence of the slip velocity on Knudsen number:

$$V_s = 8.7K_n^2 \quad (9)$$

The slip phenomena can also be discussed by using slip length ζ , which is defined as the distance between the wall and the position at which the

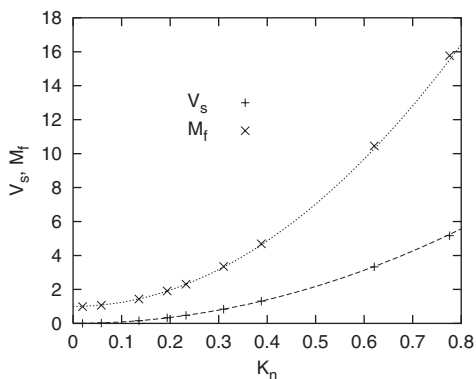


Fig. 2. The slip velocity and the normalized mass flow rate at the exit of a micro-channel flow as functions of K_n for $P_i/P_e = 2$. The “+” and “x” are LBM numerical results. The dashed and dotted lines are for theoretical predications in Eqs. (9) and (12), respectively.

extrapolated fluid velocity reaches zero. The slip length can be obtained by letting $u_y = 0$ in Eq. (8), leading to:

$$\zeta = \frac{(1 + 4V_s)^{\frac{1}{2}} - 1}{2} \quad (10)$$

As shown in Fig. 3 this result agrees well with the result obtained by a molecular dynamics approach. In the MD simulation the fluid was composed of Lennard–Jones atoms with the potential $V(r) = 4[\epsilon[(\frac{r}{\sigma})^{-12} - (\frac{r}{\sigma})^{-6}]$ and the wall–fluid interactions were modeled by a modified Lennard–Jones potential $V(r) = 16[\epsilon[(\frac{r}{\sigma})^{-12} - A(\frac{r}{\sigma})^{-6}]$ with $A = \frac{3}{8}$.⁽¹⁰⁾ In this comparison we have assumed the mean free path $l = \frac{1}{n\sigma^3}$ in order to connect the Knudsen number K_n to the normalized density $n\sigma^3$ in the molecular dynamics simulation.

If we assume that the Navier–Stokes equations are valid for the micro-flows except that (i) the traditional non-slip velocity condition on the wall is replaced by the slip boundary condition V_s using Eq. (9); (ii) the y -direction velocity is zero and the x -direction velocity is $u_0(x)(Y - Y^2 + V_s(x))$; and (iii) all the non-linearities in Eqs. (4) and (5) are negligible, then an analytic solution of the pressure distribution along the channel can be obtained:

$$(P^2 - P_e^2) + 12P_e^2 V_s \ln(P/P_e) = M_f P_e^2 (\alpha^2 - 1)(1 - X) \quad (11)$$

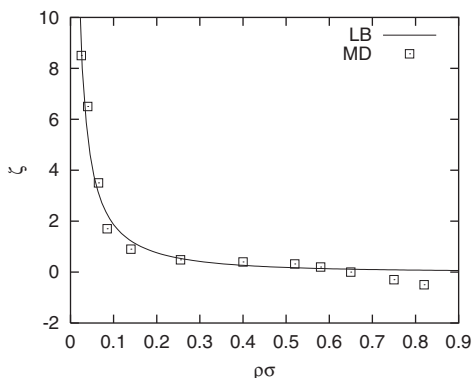


Fig. 3. The slip lengths ζ obtained by molecular dynamics approach (MD) and lattice-Boltzmann (LB) simulation as functions of normalized density $n\sigma^3$. The $l = \frac{1}{n}\sigma^3$ is used to link Knudsen number to the normalized density $n\sigma^3$ in the molecular dynamics simulation.

where $X = x/L$ and the normalized mass flow rate is

$$M_f = 1 + 12V_s(K_n) \frac{\ln(\alpha)}{\alpha^2 - 1} \tag{12}$$

For the inlet-exit pressure rate $\alpha = 2$, the above formula becomes $M_f = 1 + 24.1K_n^2$, which agrees well with the numerical results in Fig. 2.

In laminar Poiseuille flows, one usually assumes that the density variation along the channel is very small, and the pressure drop along the channel is nearly linear. In micro-channel flow, however, the ratio between the length and the width is much larger and the pressure drop is not linear. If there is no velocity slip at the walls ($V_s = 0$), according to Eq. (11),^(2,5) the pressure along the channel has the following dependence on the dimensionless coordinate:

$$P^2 = P_e^2 [1 + (\alpha^2 - 1)(1 - X)] \tag{13}$$

If the velocity at the boundaries is allowed to slip, the pressure profile along the channel will depend on the Knudsen number. In Fig. 4 we present the LBM simulation results for the normalized pressure deviation from a linear pressure profile, $(P - P_l)/P_e$, as functions of X at several Knudsen numbers, where $P_l = P_e + (P_i - P_e)(1 - X)$. It is seen that when $K_n \leq 0.2$, $(P - P_l)/P_e$ is a positive nonlinear function of X . This agrees with the results in ref. 5 using an engineering model. For $K_n \geq 0.2$, the LBM simulation shows that $(P - P_l)/P_e$ becomes negative, which is directly

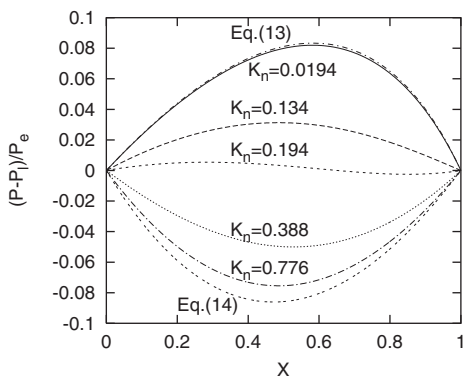


Fig. 4. The deviations from linear pressure profile for $\alpha = P_i/P_e = 2$. The top and bottom lines are the analytical results from Eq. (13) for $K_n = 0$ and Eq. (14) for $K_n \gg 1$ respectively. The other curves are LBM numerical results for the Knudsen numbers indicated.

linked to the fact that the slip velocity depends on the square of K_n in the LBM. For large K_n , the pressure can be derived from Eq. (11):

$$P = P_c[\alpha^{(1-X)}] \quad (14)$$

The negative deviation from a linear pressure distribution has not been experimentally observed before and it would be interesting to verify experimentally.

In Fig. 5 the mass flow rates as functions of the pressure ratio α when $K_n = 0.165$ are shown for our theory, the experimental work,⁽²⁾ the engineering model⁽⁵⁾ and the LBM simulation. Our theory and the LBM simulation agree well with the experimental measurements. For large pressure ratios ($\alpha \geq 1.8$), the LBM agrees reasonably well with Beskok *et al.*⁽⁵⁾ But for smaller pressure ratios, the difference increases because the dependence of the slip velocity on K_n is different among LBM and ref. 5. Beskok *et al.* have used a slip velocity model which includes linear and quadratical terms of K_n . But the linear term plays the dominating effect. Figure 5 has also included the two results from ref. 5. The upper curve uses the slip velocity which depends both linearly and quadratically on K_n . We expect that a new slip velocity formula in Eq. (9) and the Navier–Stokes equation should lead to similar results as shown in our LBM simulation.

Our second LBM numerical simulation describes two-dimensional micro-cavity flow.⁽¹¹⁾ The cavity size is $L_x = L_y = 40$ (lattice units). The upper wall moves with a constant velocity, v_0 , from left to right. The velocity boundary condition is specified using an extrapolation method. The equilibrium distributions are calculated assuming that the upper wall nodes

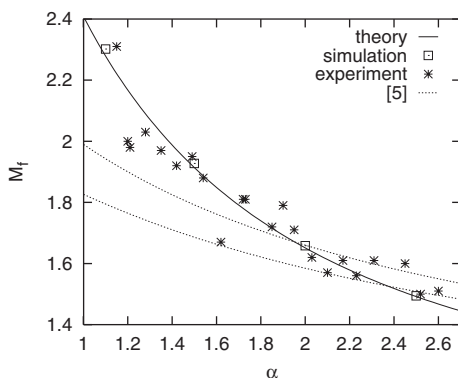


Fig. 5. The normalized mass flow rate as a function of the pressure ratio for $K_n = 0.165$. The solid line is for Eq. (12).

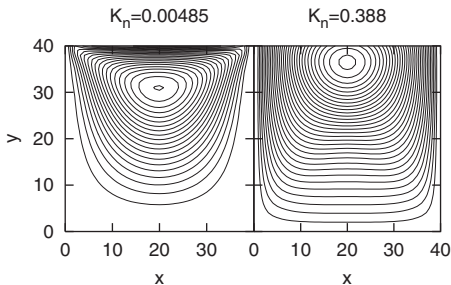


Fig. 6. Streamlines for two Knudsen numbers in the cavity flow. The upper wall of the cavity moves at a constant velocity v_0 and other three walls are still.

move at a constant velocity, v_0 . The distributions at the nodes that are just outside of the fluid are calculated using linear extrapolations. The other three walls are at rest. The boundary are set on nodes where the bounce-back boundary conditions are used. To see the dependence of flow characteristics on the Knudsen number in our simulations, we fixed the Reynolds number, $R_e = \frac{v_0 L_x}{\nu} = 2.4 \times 10^{-4}$ and require Mach number $M_a = \frac{v_0}{c_s} \leq 10^{-3}$.

In Fig. 6, we show the streamlines at two different Knudsen numbers. In Fig. 7, we show the vertical positions of the vortex center and the normalized mass flow rate between the bottom and the vortex center as functions of K_n . The normalized factor is $\rho L_x v_0$. It can be seen that at small Knudsen numbers the vortex center moves downward and the mass flow rate increases with increasing K_n . On contrast, at high Knudsen numbers the vortex center moves upward and the mass flow rate decreases with Knudsen number, which is attributed to the fact that the slip velocity on the upper wall causes momentum transfer less efficient. It has been shown

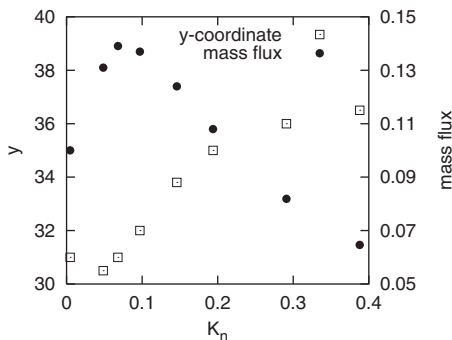


Fig. 7. The y -coordinate of the vortex center (square symbols) and the normalized mass flow rate (solid circles) between the bottom and the vortex center as a function of K_n .

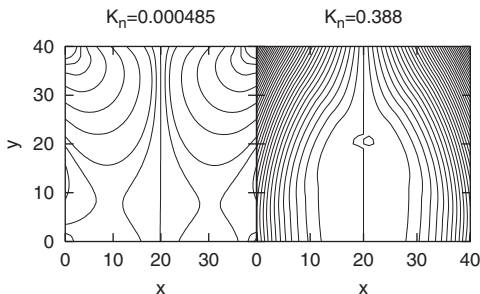


Fig. 8. The pressure contours at two Knudsen numbers as in Fig. 5.

in ref. 12 that the center of the vortex moves downward when the Reynolds number increases for very small K_n . Figure 8 shows the pressure contours for the same parameters as in Fig. 6. The pressure is calculated according to Eq. (6). Totally different pressure structures are observed in these two cases. When the Knudsen number is small, the continuum assumption is valid and the pressure contours are almost circles with centers at the upper left or the upper right corners. On the other hand, due to the slip velocity on the walls, the pressure contours become nearly straight lines for higher Knudsen numbers.

In this paper, we have used the lattice Boltzmann method to simulate the micro-channel and micro-cavity flows. Because the LBM is a kinetic method based on the particle distribution function, it can be used to study the flow dependence on Knudsen number, including the slip velocity, the nonlinear pressure drop in micro-channel and the variation of the vortex center in the micro-cavity. By comparing our simulation results with experiments we conclude that a quadratic dependence of slip velocity on Knudsen number is a better approximation. We have also discovered in high Knudsen number channel flow that negative pressure deviations from a linear pressure drop can occur, which should be verified by experiments. The LBM is especially appealing as a simulation tool for problems in MEMS due to its model simplicity and parallel efficiency.

REFERENCES

1. C. M. Ho and Y. C. Tai, Micro-electro-mechanical-systems (MEMS) and fluid flows, *Ann. Rev. Fluid Mech.* **30**:579 (1998).
2. E. B. Arkilic, M. A. Schmidt, and K. S. Breuer, Gaseous slip flow in long micro-channels, *J. MEMS* **6**:167 (1997).
3. S. A. Schaaf and P. L. Chambre, *Flow of Rarefied Gases* (Princeton University Press, Princeton, New Jersey, 1961).

4. J. Koplik and J. R. Banavar, Continuum deductions from molecular hydrodynamics, *Ann. Rev. Fluid Mech.* **27**:257 (1995).
5. A. Beskok, G. E. Karniadakis, and W. Trimmer, Rarefaction and compressibility effects in gas micro-flows, *J. of Fluids Engineering* **118**:448 (1996).
6. Shiyi Chen and Gary D. Doolen, Lattice Boltzmann method for fluid flows, *Ann. Rev. Fluid Mech.* **30**:329 (1998).
7. Y. H. Qian, D. d'Humières, and P. Lallemand, Lattice BGK models for Navier–Stokes equation, *Europhys. Lett.* **17**:479 (1992).
8. H. Chen, S. Chen, and W. H. Matthaeus, Recovery of the Navier–Stokes equations using a lattice gas Boltzmann method, *Phys. Rev.* **A45**:R5339 (1992).
9. S. Y. Chen, D. Martinez, and R. W. Mei, On boundary conditions in lattice Boltzmann methods, *Phys. Fluids* **8**(9):2527 (1996).
10. M. Cieplak, Joe Koplik, and J. R. Banavar, Boundary conditions at fluid-solid interface, *Phys. Rev. Lett.* **86**:803 (2001).
11. G. K. Karniadakis, S. A. Orszag, E. M. Ronquist, and A. T. Patera, Spectral element and lattice gas methods for incompressible fluid dynamics, in *Compressible Computational Fluid Dynamics*, M. D. Gunzburger and R. A. Nicolaides, eds. (Cambridge University Press, 1993).
12. Shuling Hou, Qisu Zou, Shiyi Chen, Gary Doolen, and Allen C. Cogley, Simulation of incompressible Navier–Stokes fluid flows using a lattice Boltzmann method, *J. Comput. Phys.* **118**:329 (1995).